Material Characterization and the Formation of Nanoporous PMSSQ Low-K Dielectrics

P. Lazzeri[1], L. Vanzetti[1], E. Iacob[1], M. Bersani[1], M. Anderle[1], J.J. Park[2], Z. Lin[2], R.M. Briber[2], G.W. Rubloff[2], R.D. Miller[3]

[1] *ITC-irst, via Sommarive 18, 38050 Povo, Trento, Italy*
[2] *University of Maryland, 2145 A.V. Williams Building, College Park, MD 20742-3285, USA*
[3] *IBM Almaden Research Center, 650 Harry Road, San Jose, CA 95120-6099, USA*

Abstract. A novel metrology strategy has been developed and applied to characterize the complex chemical transformations which are required to form spin-cast nanoporous low-K materials. Surface analysis based on Time-of-Flight Secondary Ion Mass Spectrometry (ToF-SIMS) has been applied in static and dynamic modes, and coupled with X-ray Photoemission Spectroscopy (XPS), to observe the compositional and chemical bonding changes of the surface and the underlying thin film. Results show the cross-linking of the low-K matrix as a function of thermal processing, along with details of the evolution of porogen species that provide the template for forming nanovoids in the fully-processed material. This approach is promising more generally for characterizing materials transformations, particularly those involving polymeric systems where ToF-SIMS analysis of large molecular fragments represents a highly specific analytical tool.

INTRODUCTION

The introduction of low-K materials as interconnection dielectrics in the manufacturing of next generation ULSI devices [1] is very challenging, both in achieving the required material properties and in satisfying the demands of process integration [2,3]. Both spin-on and plasma CVD approaches are being actively pursued to achieve low-K dielectrics [4]. Spin-on approaches have advantages for realizing lower intrinsic dielectric constants and because chemical synthesis offers many options for such polymeric systems. Moreover, a further reduction of K can be obtained by introducing porosity in these materials.

Porosity can be obtained by adding a sacrificial porogen to the dielectric precursor material [5,6]. After the precursor material is spin-cast, it is subjected to thermal curing to promote the polymerization of the dielectric resin. During the curing cycle, the porogen species undergo transformations, degradation, and volatilization. If properly engineered, the materials choice and curing process solidify a cross-linked low-K matrix around porogen nanoparticles, and afterwards the porogen material is degraded to leave a network of nanopores in a rigid low-K dielectric matrix.

While this preparation method appears simple, the occurrence of the concurrent reactions going on during the curing treatment has a major impact on the properties of the porous low-K dielectric. The mechanical and electrical characteristics of the low-K material are in fact influenced by the size, the density and the features of the pores that, in turn, are related to the polymerization kinetics of the dielectric resin and to the degradation process of the porogen. As a consequence, the investigation of the transformations going on during the formation of these materials is crucial for the development and manufacturing of porous low-K dielectrics.

To meet the challenge of characterizing and understanding these complex phenomena, a metrology strategy based on ToF-SIMS and XPS has been developed to evaluate the transformations occurring during the formation of spin-on porous dielectrics. Low-K materials based on polymethylsilsesquioxane (PMSSQ) and containing polymethylmethacrylate-dimethylaminoethylmethacrylate copolymer (PMMA-co-DMAEMA) as porogen were chosen for this purpose because of their current high industrial interest. To evaluate the polymerization kinetics of the dielectric resin and to investigate the degradation mechanisms of the porogen, several analytical approaches were attempted.

EXPERIMENTAL

Two different PMSSQ precursors were used for the preparation of the amorphous silica-based nanoporous low-K dielectrics. One had a lower initial

functionality (termed "low-SiOH" hereafter) than the other (termed "high-SiOH). Both precursors were mixed with the same amount of PMMA-co-DMAEMA porogen (30% by weight) prior to spin-casting. Fully deuterated PMMA copolymerized with conventional DMAEMA was used as porogen in low-SiOH material in order to more precisely elucidate the chemical transformations of these materials. About 0.5 μm thick films were deposited using these solutions on two sets of 1" wafers by spin coating. The samples then underwent a low temperature (50°C) annealing under N_2 atmosphere to remove the solvent. Afterward, they were cured at progressively higher temperatures under N_2 atmosphere as shown in table 1.

TABLE 1. Sample ID [a].

Sample ID	Curing T [°C]	Curing t [min]	Porogen
1-low-SiOH / 1-high-SiOH	50	3 / 2	NO
2-low-SiOH / 2-high-SiOH	50	3 / 2	D-p / C-p
3-low-SiOH / 3-high-SiOH	125	60	D-p / C-p
4-low-SiOH / 4-high-SiOH	175	60	D-p / C-p
5-low-SiOH / 5-high-SiOH	225	60	D-p / C-p
6-low-SiOH / 6-high-SiOH	275	60	D-p / C-p
7-low-SiOH / 7-high-SiOH	325	60	D-p / C-p
8-low-SiOH / 8-high-SiOH	450	120	D-p / C-p

Positive and negative static SIMS (SSIMS) spectra were acquired from these samples by a ToF-SIMS instrument (ION-TOF, ToF-SIMS IV) using a pulsed 11 keV Ga^+ primary beam. In addition, SIMS spectra were acquired after sputtering the material with a 10 keV Cs^+ beam and using a 25 keV Ga^+ beam for the sampling of the newly exposed surface (termed "pseudo-DSIMS measurements" hereafter). The mass resolution under these experimental conditions was 5000 @ $^{28}Si^+$ and 4000 @ $^{16}O^-$. XPS measurements were carried out by using a Scienta ESCA 200 instrument equipped with a monochromatic Al Kα source. The spectra were collected at 90° emission angle (normal to the surface) with energy resolution of 0.4 eV. XPS analyses were also performed after sputtering the samples by a 3 keV Ar^+ beam. Within these experimental conditions, the information depth is approximately 8-10 nm. SSIMS and XPS spectra were also acquired after etching the samples for 5 sec. in 0.5 % HF solution.

RESULTS AND DISCUSSION

PMSSQ polymerization kinetic

The evaluation of the PMSSQ polymerization kinetics relies on the intensity measurement of several

---

[a] D-p : porogen with deuterated PMMA; C-p: conventional porogen

key peaks characterizing the SSIMS spectra of the precursor materials.

As pointed out by a detailed spectroscopic investigation of the SSIMS data discussed elsewhere [7], these peaks are due to series of molecular ions containing an increasingly high number of Si atoms, a suitable number of O atoms, and methyl groups, so that it can be argued that they are related to the PMSSQ oligomers. The mass and conjectured composition of the key species is summarized in table 2.

TABLE 2. Conjectured composition, SSIMS key peaks.

Negative SSIMS		Positive SSIMS	
measured mass [amu]	conjectured composition	measured mass [amu]	conjectured composition
134.96	$Si_2O_4CH_3$		
194.92	$Si_3O_6CH_3$	198.98	$Si_3O_4C_3H_9$
268.94	$Si_4O_7C_3H_9$	252.94	$Si_4O_6C_3H_9$
342.97	$Si_5O_8C_5H_{15}$	329.67	$Si_5O_7C_5H_{15}$
402.92	$Si_6O_{10}C_5H_{15}$	386.93	$Si_6O_9C_5H_{15}$
476.95	$Si_7O_{11}C_7H_{21}$	460.95	$Si_7O_{10}C_7H_{21}$
536.91	$Si_8O_{13}C_7H_{21}$	520.92	$Si_8O_{12}C_7H_{21}$
610.93	$Si_9O_{14}C_9H_{27}$	594.94	$Si_9O_{13}C_9H_{27}$

The intensity of the key peaks is observed to progressively decrease in the spectra of the (partially) cured materials. In addition, unique features that can be ascribed to the different functionality of the precursor materials are clearly highlighted by the SSIMS fingerprints [7].

The intensity decrease of the key peaks with annealing is shown by all the species listed in table 2 in both sets of samples. This behavior can be easily explained by taking into account that the polymerization of the PMSSQ correspondingly causes the disappearance of the oligomers. It is believed therefore that the intensity measurements of the key peaks provide a signature of the curing and cross-linking process which may lead to a quantitative metrology for representing the degree of matrix reconfiguration. These outcomes should enable benefits from both the manufacturing and technology points of view. Nevertheless, the quantitative estimation of matrix reconfiguration must rely on consistent data for the absolute intensity of the peaks. A statistically relevant number of SSIMS spectra were thus acquired to enhance the reliability of the measurements, along with optimization of experimental parameters for the ToF-SIMS measurements and analysis. Using these conditions, the signal intensity of the elemental ions related to the MSSQ (i.e. Si, O, SiO_2) was observed to be closely similar for all the spectra acquired from samples #1 to #7. Indeed, the signal intensity systematically increased in the spectra from samples #8, due to the loss of porogen and corresponding augmentation of the MSSQ concentration (see discussion below). Using

these experimental datasets, the intensity variation of the key species was evaluated. The results obtained by the high-SiOH set of samples are shown in fig. 1, which shows the intensity of the key positive ions as a function of the intensity of the negative ions [7] likely related to the same species (the corresponding ions lie on the same row in table 2).
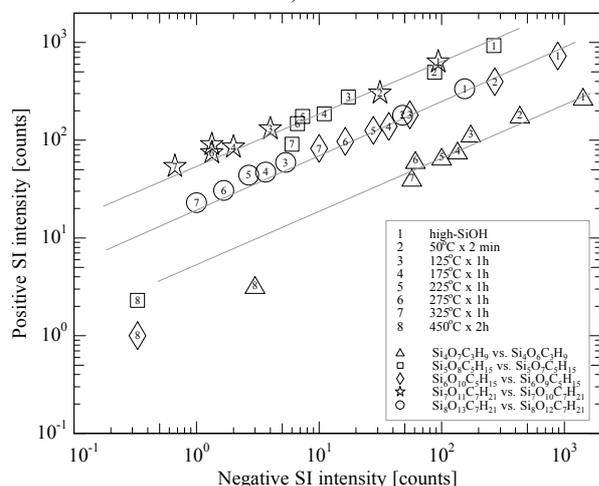

Figure 1. Key peaks intensity (pos. vs. neg. SI)

From this plot, it can be readily observed that the vanishing of the positive species is accompanied by a proportional intensity decrease for the corresponding negative ions. All the points, with the only exception of the data referred to samples #8, lie very close to equivalent straight lines. The slope of the lines is the same, revealing that an identical correlation function is suitable to fit the variation of the peak intensities, regardless of the mass of the species. Moreover, the slope of the lines is less than 1. This indicates that the detection of the negative species is favorable, as the range of the intensity variation is less for the positive ions. The scattering of the few data points related to sample #8 is simply due to peak intensities being low or close to zero for this case.

As shown by fig. 1, the highest peak intensity is measured for sample #1. Accordingly, this sample is expected to have the largest oligomers concentration, since it is not cured and does not contain porogen. The intensity of key species then decreases as the polymerization of the PMSSQ precursors proceeds, reaching the lowest value for sample #8. Analogous conclusions are provided by the low-SiOH samples, confirming that the proportional intensity variation of the key species is a systematic experimental reflection of the behavior of the material. In addition, while a proportional intensity variation is shown by all the paired ions, the relative intensity variation for the larger species appears greater than the variation of the smaller ones. Although further investigations are required to clarify this point, these results certainly

demonstrate that a quantitative relationship relates the SSIMS peak intensities and PMMSQ oligomers concentration. Accordingly, the intensity variation of the key species as measured by sampling the low-SiOH and high-SiOH materials is noticeably different. This is shown by fig. 2, where the intensity of several key species as measured by the two set of samples is displayed.
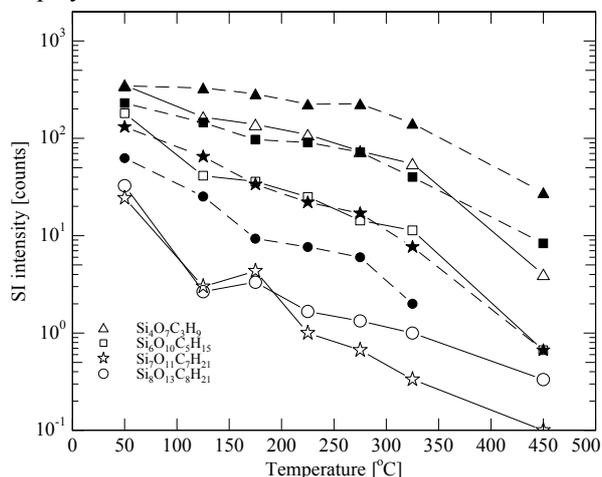

Figure 2. Key peaks intensity in low-SiOH (filled symbols) and high-SiOH (open symbols) vs. curing temperature.

Figure 2 shows that as soon as the precursors are annealed, the intensity of the key peaks diminishes. It must be noted however, that the relative key peaks intensity variation is greater for the high-SiOH material. This behavior suggests that the polymerization goes on faster if the precursor has a higher initial functionality. On the other hand, a partial intensity drop already occurred upon curing the high-SiOH precursor around 125°C, indicating that the cross-linking is promoted as soon as the annealing temperature is in excess of 50°C. The decrease of the peak intensities continues, and finally a net reduction is observed upon annealing at 450°C. A similar behavior is shown by the low-SiOH material, but the key peaks intensity decreases more slowly. Consequently, for each annealing treatment the degree of curing of the high-SiOH PMSSQ is larger than that of the low-SiOH material. Analogous results were obtained by sampling the HF etched samples. Also in this case, a proportional relationship was observed to characterize the intensity decrease of the pos. and neg. species, thus confirming that the evaluation of the PMSSQ polymerization as based on the surface or dielectric bulk characterization leads to similar conclusions.

Porogen degradation mechanism

To characterize the kinetics of the nanoporous PMSSQ material, it is also important to observe and

measure signatures of changes and volatilization of the PMMA-co-DMAEMA porogen, which is also revealed in the SSIMS spectra. However, this raises the question of whether the surface concentration of porogen species is indeed representative of that in the underlying thin film.

XPS clearly revealed that the amount of porogen on the surface of the low-SiOH samples was lower than expected, in particular as observed in comparison of the spectra prior to and after Ar^+ sputtering. Even though chemical state information is disrupted by sputtering the material, compositional indications are still valid. It was thus observed that the nitrogen concentration, associated directly with the DMAEMA ligand is about three times higher in the film than on the surface. Complementary analytical schemes based on ToF-SIMS were thus tested to develop a generally applicable procedure for the detection of porogen, regardless of its amount on the surface. To this end, the near-surface region of the materials was investigated after using ion beam sputtering for the removal of the uppermost layers of the low-K films. For the development of this methodology, the low-SiOH samples containing deuterated porogen were used.

As stated in [7], various markers related to the porogen can be recognized by studying the pseudo-DSIMS spectra of the low-SiOH samples. The more important among them are listed in table 3. Interestingly, in spite of the molecular fragmentation induced by the sputtering beam, some of these markers can still be correlated to the various part of the PMMA-co-DMAEMA molecule (i.e. PMMA ligand, DMAEMA ligand, copolymer backbone).

TABLE 3. Porogen markers (neg. SI, pseudo-DSIMS)

PMMA ligand		DMAEMA ligand		backbone
D	OD	CN	C_3N	$C_3 - C_9$
CD	COD_3	C_2N	CNO	

Upon curing, the intensity of the porogen-related species varies in a distinctive fashion. In particular, the intensity of the markers related to the DMAEMA ligand decreases by about a factor of 10 upon annealing at 225-275 °C. In contrast, the intensity of the markers related to the PMMA ligand and porogen backbone is stable up to annealing the material at 325 °C. Upon the treatment at 450 °C however, the intensity of all the porogen markers is observed to drop to the background value.

The two sets of PMSSQ samples were also analyzed by XPS. The core levels O 1s, C 1s, Si 2p, N 1s were acquired and the percentage of each element was calculated for these materials using known [8] atomic sensitivity factors. The semiquantitative XPS results are summarized in table 4. In figure 3, the C 1s core level is shown for pairs of representative samples.

TABLE 4. Semiquantitative composition of high-SiOH and low-SiOH materials (based on XPS)

Sample ID	O %	C %	Si %	N %
1-low-SiOH	37.6	27.1	35.2	- / -
1-high-SiOH	40.1	25.0	34.9	
2-low-SiOH	36.0	34.6	28.9	0.47
2-high-SiOH	37.1	36.1	26.4	0.44
3-low-SiOH	35.1	35.6	28.9	0.46
3-high-SiOH	36.6	36.5	26.5	0.45
4-low-SiOH	35.6	33.8	30.2	0.44
4-high-SiOH	35.9	36.6	27.1	0.46
5-low-SiOH	36.0	32.7	31.1	0.24
5-high-SiOH	36.9	34.2	28.7	0.24
6-low-SiOH	35.7	33.8	30.5	- / -
6-high-SiOH	35.8	36.3	27.9	
7-low-SiOH	36.0	33.4	30.7	- / -
7-high-SiOH	36.0	35.0	29.0	
8-low-SiOH	36.6	27.9	35.5	- / -
8-high-SiOH	42.7	18.9	38.5	

Several things are evident from these data. In particular, the two sets of samples are different. Besides, the amount of nitrogen decreases upon curing at 225-275 °C.
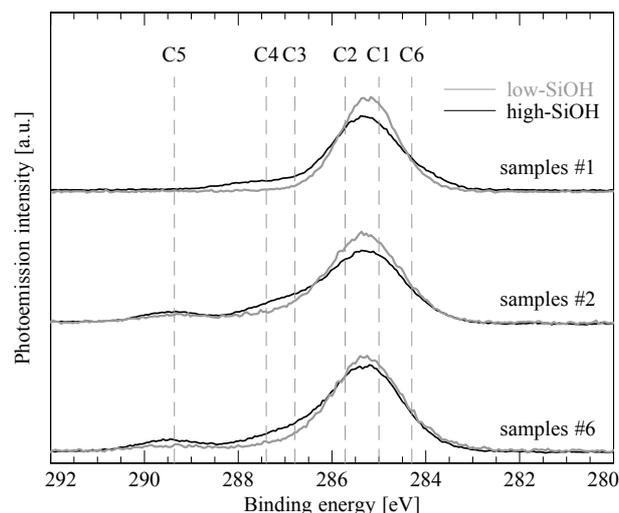

Figure 3. Evolution of C1s peak upon curing.

The deconvolution of the C 1s peak shows that samples 1-low-SiOH and 1-high-SiOH (top spectra in fig. 3) can be fitted with 3 and 4 peaks, respectively. This difference is still clearly visible in the other examples (middle and bottom spectra in fig. 3) but here additional peaks are present that are due to the porogen. In particular, the carbon peak deconvolution leads to the identification of 6 peaks, named C_1 to C_6, that have been assigned [9] to the following bonding: C_1:CH; C_2:C-C; C_3:C-OH or C-N; C_4:C=O; C_5:O=C-OH; C_6:C-Si. The features revealed by the top spectra in fig. 3 are likely related to the characteristic functionality of the two precursors. C_3 and C_5 can be related to the porogen, that has C_1 and C_2 type of bonding as well. These peaks evolve with temperature

in both sets of samples and finally disappear upon annealing at T > 325 °C.

The thermally-induced evolution of the porogen reflects the thermal stability of the different molecular moieties from which the porogen is composed. Based on these results, it can thus be argued that the degradation of the copolymer involves the partial cleavage of the DMAEMA ligand first. The byproducts of this reaction must be released by the material, as both XPS and ToF-SIMS detect a clear decrease of N concentration or signal drop of the pseudo-DSIMS markers related to DMAEMA. The largest amount of residual porogen however, mainly constituted by PMMA and copolymer backbone, does not undergo degradation until the annealing temperature is in excess of 325 °C. At this point, the volatile byproducts formed by this degradation are released from the material. Accordingly, the intensity of C_3 and C_5 XPS peaks as well as the pseudo-DSIMS markers related to the residual porogen decrease. These conclusions are confirmed by thermal desorption investigations of bulk copolymers reported in [10,11]. As a consequence of the final porogen degradation, the materials are primarily composed of only MSSQ. For this reason, the SSIMS signal intensity of the elemental ions related to MSSQ, as well as the Si content as measured by XPS, is higher in the spectra from samples #8.

CONCLUSIONS

The overall transformations leading to the formation of the PMSSQ-based low-K dielectrics are summarized in fig. 4. In this plot, selected ToF-SIMS signals representative of the matrix and porogen species are shown. From figure 4 it can be readily seen that the temperature ranges for polymerization of the PMSSQ precursors and the degradation of the porogen overlap significantly. Moreover, one might expect the high-SiOH material to display more substantial chemical change upon curing, since matrix cross-linking is intimately associated with functionality. Thus, the data in fig. 4 demonstrate clearly that the two materials behave quite differently. Given that the relation of matrix cross-linking to porogen evolution is critical in determining nanopore structure, this means that the two materials should have notably different technological performance.

Indeed, we have observed large porogen aggregates (about 1 μm in diameter) from curing of the low-SiOH precursor, which may be associated with the slower polymerization of this material. Conversely, a completely different behavior is shown by the high-SiOH material, without evidence for such porogen aggregation.
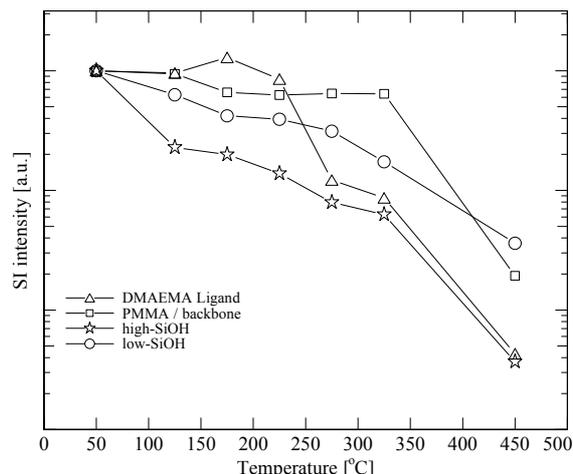

Figure 4. Overall materials transformation (based on ToF-SIMS markers).

There results reveal substantial information about the processes of PMSSQ polymerization and porogen reaction and volatilization as a function of thermal treatment, key issues for producing high quality nanoporous low-K dielectrics by well documented and controllable processes suitable for semiconductor manufacturing. Accordingly, the value of ToF-SIMS and XPS in addressing such complex reactive nanosystems is clearly seen.

ACKNOWLEDGEMENTS

REFERENCES

[1] *The International Technology Roadmap for Semiconductors*, Semiconductor Industry Association, Santa Clara (CA, USA), 2001, Interconnect
[2] Yu K.C. et al., "Integration Challenges of 0.1 μm CMOS Cu/Low-k Interconnects", *Proc. Int'l. Interconnect Technology Conf. 2002*, ed. by IEEE Electron Devices Society, Omnipress, Madison (WI, USA), 2003
[3] Hayashi Y., *ibidem*
[4] Peters L., *Semiconductor International*, **9** (1998)
[5] Miller R.D., Hedrick J.L., Yoon D.Y., Cook R.F., Hummel J. P., *MRS Bulletin*, **22**, 44 (1997).
[6] Huang Q., Frank C.W., Mecerreyes D., Miller R.D., *Polymer Materials: Science & Engineering*, **84**, 792 (2001).
[7] Lazzeri P., Vanzetti L. Rubloff G.W., Briber R.M., Anderle M., Miller R.D., Bersani M. Lin Z., Park J.J. Appl. Surf. Sci. (submitted)
[8] Scienta ESCA 200 database
[9] Beamson G., Briggs D., *High Resolution XPS of Organic Polymers*, John Wiley & Sons, Chichester (England), 1992
[10] Huan K., Bes L., Haddleton D.M, Khoshdel E., *J. Polym. Sci.* A, **39**, 1833-1842 (2001)
[11] Czégény Z., Iakab E., Blaszó, *Macromol. Mater. Eng.*, **287 (4)**, 277-284 (2002)